Dalton Transactions

Accepted Manuscript

ROYAL SOCIETY OF CHEMISTRY

www.rsc.org/dalton

Cite this: DOI: 10.1039/c0xx00000x

www.rsc.org/xxxxxx

ARTICLE TYPE

Synthesis and electrochemistry of β-pyrrole nitro-substituted cobalt(II) porphyrins. Effect of the NO_2 group on redox potentials, electron transfer mechanism and catalytic reduction of molecular oxygen in acid media

Bin Sun,[a] Zhongping Ou,*[a] Shuibo Yang,[a] Deying Meng,[a] Guifen Lu,[a] Yuanyuan Fang[b] and Karl M. Kadish*[b]

Received (in XXX, XXX) Xth XXXXXXXXX 20XX, Accepted Xth XXXXXXXXX 20XX
DOI: 10.1039/b000000x

Abstract: Four cobalt(II) porphyrins, two of which contain a β-pyrrole nitro substituent, were synthesized and characterized by electrochemistry and spectroelectrochemistry. The investigated compounds are represented as (TRPP)Co and (NO_2TRPP)Co, where TRPP is the dianion of a substituted tetraphenylporphyrin and R is a CH_3 or OCH_3 substituent on the four phenyl rings of the macrocycle. Two reductions and three oxidations are observed for each compound in CH_2Cl_2 containing 0.10 M tetra-*n*-butylammonium perchlorate. The first reduction of the compounds without a nitro substituent is metal-centered and leads to formation of a Co(I) porphyrin which then reacts with the CH_2Cl_2 solvent to generate a carbon σ-bonded Co^{III}-R complex. A further reduction then occurs at more negative potentials to generate an unstable Co(II) σ-bonded compound. In contrast to these reactions, the first reduction of the nitro-substituted porphyrins is macrocycle-centered under the same solution conditions and gives a Co(II) porphyrin π-anion radical product. This reversible electron transfer is then followed at more negative potentials by a second reversible one-electron addition to give a Co(II) dianion. Three reversible one-electron oxidations are also seen for each compound. The first is metal-centered and the next two involve the conjugated π-system of the macrocycle. Each neutral Co(II) porphyrin was also examined as to its catalytic activity for electoreduction of molecular oxygen when coated on an edge-plane pyrolytic graphite electrode in 1.0 M $HClO_4$. The β-pyrrole nitro-substituted derivatives were shown to be better catalysts than the non-nitro substituted compounds under the utilized experimental conditions.

Introduction

Porphyrins and porphyrin analogues have attracted considerable attention for use in a broad range of applications[1,2] because of their versatile properties, derived in part from their stable π-ring system, in part from the nature of the substituents on the meso and/or β-positions of the macrocycle and in part from the coordinating ability of the central metal ion which can exist in a variety of oxidation states.

Previous electrochemical characterization of porphyrins with redox inactive M(II) and M(III) central metal ions have shown that the presence of one or more electron-withdrawing NO_2 groups at the meso- or β-pyrrole positions of the conjugated macrocycle will have a large effect on the half-wave potentials for electroreduction. The reversible $E_{1/2}$ values of metallated tetraphenylporphyrins, (TPP)M, have been shown to shift in a positive direction by 230-380 mV per nitro group in the case of β-pyrrole substituted nitro derivatives and by 450-550 mV in the case of *meso*-substituted nitro derivatives of octaethylporphyrins, (OEP)M.[3] When an NO_2 substituent is located on the phenyl ring of a TPP type porphyrins,[4,5] on the quinoxaline group of a quinoxalino- porphyrin,[6] or on the phenyl group of a triphenylcorrole,[7-9] it can be reversibly reduced by one-electron in nonaqueous media. However, a direct reduction of this electron-withdrawing group does not occur in non-aqueous media when this group is directly attached at the *meso* or β-pyrrole positions of a porphyrin macrocycle; the main effect of NO_2 in this case is to positively shift $E_{1/2}$ for the oxidation and reduction.

In a few cases, the incorporation of NO_2 into the porphyrin macrocycle has been shown to change the site of electron transfer from a metal-centered to a macrocycle-centered reduction, two examples being given for $[(NO_2)P]Au^{III}PF_6$[10] and $[(NO_2)TRPP]Fe^{III}Cl$,[11] where P and TRPP are the dianions of 5,10,15,20-tetrakis(3,5-di-tert-butylphenyl)porphyrin and a substituted tetraphenylporphyrin, respectively, and R represents one CH_3 or two OCH_3 groups on each phenyl ring of the TRPP macrocycle. Finally, it has been well-documented in the literature that NO_2 substitution at the β-pyrrole or meso-position of a TPP or OEP type complexes has a much smaller effect on $E_{1/2}$ for oxidation than on the half-wave potentials for reduction.[4]

Our own laboratories have recently demonstrated that the type of substituents on the *meso*-phenyl rings of a porphyrin or related corrole macrocycle can have a significant effect on the compound's catalytic properties for reduction of molecular oxygen in acid media.[7,12,13] However, to the best of our knowledge, it is still not known how a single strong electron-withdrawing NO_2 substituent on the β-pyrrole position of a cobalt porphyrin will affect the electrocatalytic activity of these types of

compounds when adsorbed on an electrode surface. This is investigated in the present paper where we have synthesized and characterized two β-pyrrole NO_2-substituted Co(II) porphyrins and the related non-nitro substituted Co(II) porphyrins (see Chart 1). The electrochemical properties of these compounds were examined in nonaqueous media and the effect of the β-nitro group on the UV-visible spectra and reduction/oxidation properties are discussed with comparisons made to the non-nitro substituted porphyrins containing the same central metal ions. The catalytic activity of these porphyrins towards the reduction of molecular oxygen in acid media was also evaluated by utilizing cyclic voltammetry and linear sweep voltammetry at a rotating disk electrode (RDE).

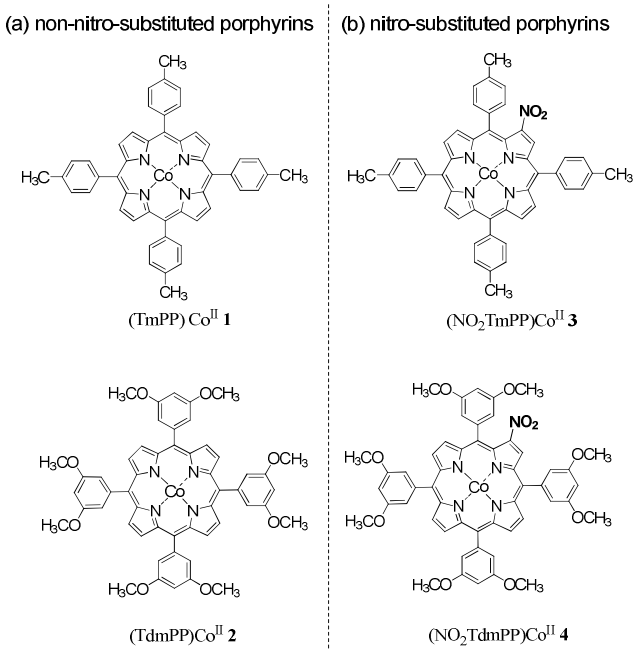

Chart 1. Structures of investigated cobalt porphyrins.

Experimental

Materials and instrumentation

Reagents and solvents (Sigma-Aldrich, Fluka or Sinopharm Chemical Reagent Co.) for synthesis and purification were of analytical grade and used as received. Dichloromethane (CH_2Cl_2, 99.8%) was purchased from Sinopharm Chemical Reagent Co. and distilled before use. Tetra-*n*-butylammonium perchlorate (TBAP) was purchased from Sigma Chemical or Fluka Chemika Co., recrystallized from ethyl alcohol, and dried under vacuum at 40 ^{o}C for at least one week prior to use.

Thin-layer UV-visible spectroelectrochemical experiments were performed with a home-built thin-layer cell which has a light transparent platinum net working electrode. Potentials were applied and monitored with Chi-730C Electrochemical Work Station. Time-resolved UV-visible spectra were recorded with a Hewlett-Packard Model 8453 diode array spectrophotometer. High purity N_2 was used to deoxygenate the solution and kept over the solution during each electrochemical and spectroelectrochemical experiment. Infrared spectra were recorded with Nicolet Nexus 470. MALDI-TOF mass spectra were carried out on a Bruker BIFLEX III ultrahigh resolution.

All electrochemical measurements were carried out with a Chi-730C Electrochemical Work Station. A three-electrode system was used and consisted of glassy carbon working electrode for regular cyclic voltammetry, an edge-plane pyrolytic graphite (EPPG) disk working electrode (Model MT134, Pine Instrument Co.) for cyclic voltammetry and linear sweep voltammetry at an RDE and a platinum net working electrode for in situ spectroelectrochemistry. A platinum wire served as the auxiliary electrode and a saturated calomel electrode (SCE) as the reference electrode, which was separated from the bulk of the solution by means of a salt bridge. The potential of the SCE is 0.241 V vs NHE.

A Pine Instrument MSR speed controller was used for the RDE experiments. The catalysts were irreversibly adsorbed on the electrode surface by means of a dip-coating procedure.[14] The freshly polished electrode was dipped in a 1.0×10^{-3} M catalyst solution of CH_2Cl_2 for 5s, transferred rapidly to pure CH_2Cl_2 for 1-2s, and then exposed to air where the adhering solvent rapidly evaporated leaving the porphyrin catalyst adsorbed on the electrode surface.

Synthesis

Free-base porphyrins. $(TRPP)H_2$ and $(NO_2TRPP)H_2$ were prepared according to previously described procedures.[11,15]

Cobalt porphyrins. The corresponding free-base porphyrin (~30 mg) and 10 equivalents cobalt acetate were dissolved in N,N'-dimethylformamide. The solution was then stirred and heated to reflux. After 1.5 h the solvents were removed and the crude products chloromatographed using neutral alumina (200-300 mesh) and CH_2Cl_2/hexane as eluent. The red fraction was collected and evaporated to dryness, yielding the pure desired compounds, (TmPP)Co, (NO_2TmPP)Co, (TdmPP)Co and (NO_2TdmPP)Co, where TmPP and TdmPP are dianions of a substituted tetraphenylporphyrin, m represents a CH_3 group and dm represents two OCH_3 substituents on each of the four phenyl rings of the macrocycle.

(TmPP)Co **1**. Yield 95%. UV-vis (CH_2Cl_2): λ_{max}, nm (logε) 410 (5.51), 529 (4.48). IR (KBr): cm^{-1} 1000 ($\nu_{N\text{-}Co}$). MS(MALDI-TOF): m/z 729.35, calcd. for $[M+2H]^+$ 728.77.

(TdmPP)Co **2**. Yield 90%. UV-vis (CH_2Cl_2): λ_{max}, nm (logε) 412 (5.48), 527 (4.23). IR (KBr): cm^{-1} 1004 ($\nu_{N\text{-}Co}$). MS (MALDI-TOF): m/z 913.26, calcd. for $[M+2H]^+$ 912.87.

(NO_2TmPP)Co **3**. Yield 86%. UV-vis (CH_2Cl_2): λ_{max}, nm (logε) 380 (4.43), 424 (4.91), 542 (3.89), 575 (3.79). IR (KBr): cm^{-1} 1523, 1345 (ν_{NO2}), 1003 ($\nu_{N\text{-}Co}$). MS (MALDI-TOF): m/z 774.03, calcd. for $[M+2H]^+$ 773.77.

(NO_2TdmPP)Co **4**. Yield 86%. UV-vis (CH_2Cl_2): λ_{max}, nm (logε) 382 (4.55), 427 (5.06), 539 (4.00), 580 (3.91). IR (KBr): cm^{-1} 1520, 1351 (ν_{NO2}), 1008 ($\nu_{N\text{-}Co}$). MS (MALDI-TOF): m/z 958.19, calcd. for $[M+2H]^+$ 957.87.

Results and discussion

Synthesis

Cobalt(II) porphyrins were synthesized by reaction of the corresponding free-base porphyrin and cobalt acetate. The

progress of the reaction was monitored by thin-layer chromatography (tlc). A high yield of the porphyrin was obtained (86-95%) and the purity was confirmed by UV-visible spectroscopy and mass spectrometry.

UV-visible spectra

UV-visible spectra of the cobalt porphyrins were measured in CH_2Cl_2 and are illustrated in Fig. 1. As seen in this figure, the non-nitro substituted porphyrins, (TmPP)Co **1** and (TdmPP)Co **2** exhibit a sharp Soret band at 410-412 nm and a weak Q band at 527-529 nm. Almost identical UV-visible spectra are seen for **1** and **2**, indicating that the change of substituents on the four *meso*-phenyl rings of the macrocycle from CH_3 to OCH_3 have only a small effect on the spectra. In contrast, significant spectral differences are seen between the β-pyrrole nitro-substituted porphyrins **3** and **4** and their non-nitro substituted parent derivatives **1** and **2**. The nitro-substituted porphyrins **3** and **4** are characterized by a broad Soret band at 424-427 nm and a shoulder at 380-382 nm. There are also two Q bands between 539-580 nm as seen in Fig. 1. The broading of the bands and the 12-15 nm red-shift for compounds **3** and **4** as compared to **1** and **2** is as expected due to addition of the strong electron-withdrawing NO_2 group on the β-pyrrole position of the porphyrin macrocycle.

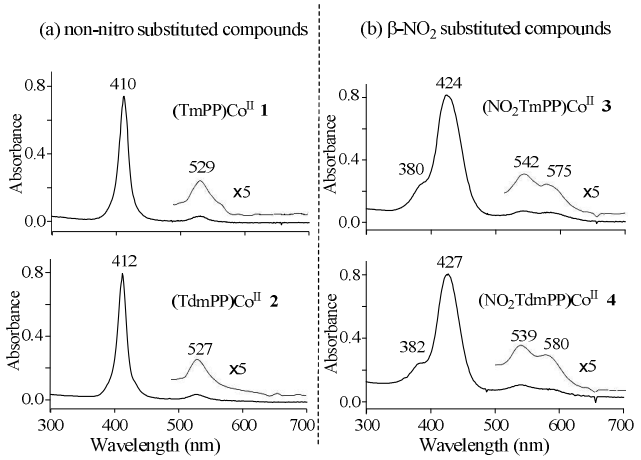

Fig.1. UV-visible spectra of (a) the non-nitro substituted porphyrins **1**, **2** and (b) the β-pyrrole NO_2-substituted cobalt porphyrins **3** and **4** in CH_2Cl_2.

Electrochemistry

The electrochemical properties of each complex were examined in CH_2Cl_2 containing 0.10 M TBAP. Examples of cyclic voltammograms for compounds **1** and **3** are illustrated in Fig. 2 and a summary of the half-wave or peak potentials for all four cobalt porphyrins is given in Table 1.

Three reversible one-electron oxidations are seen for each porphyrin in CH_2Cl_2 containing 0.10 M TBAP. This redox behavior is similar to that for other cobalt tetraphenylporphyrins containing electron-donating or electron-withdrawing substituents on the *meso* and/or β-pyrrole positions of the macrocycle and is unique to CH_2Cl_2 where all three processes are reversible.[3]

The first oxidation of compound **1** is located at $E_{1/2}$ = 0.72 V while the second and third oxidations are located at $E_{1/2}$ = 0.96 V and 1.15 V, respectively. Compound **3** is harder to oxidize than compound **1** and the $E_{1/2}$ values are shifted to 0.80, 1.05 and 1.28 V. Thus the positive shift in half-wave potentials due to the addition of the one nitro group to the conjugated π-system of the macrocycle is 80 mV for the first oxidation, 90 mV for the second and 130 mV for the third. This is consistent with the first oxidation being a metal-centered process and leading to a Co(III) porphyrin and the last two processes being porphyrin ring-centered to give a Co(III) π-cation radical and dication, respectively.[3] The same relative magnitude of shift in $E_{1/2}$ is seen when comparing $E_{1/2}$ values for compounds **2** and **4** and the same sites of electron transfer are proposed to occur upon oxidation as described above. This was confirmed by *in-situ* thin-layer UV-visible spectroelectrochemical measurements described on the following pages.

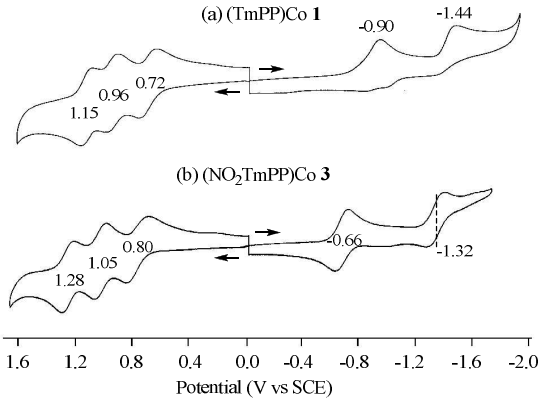

Fig. 2. Cyclic voltammograms of (a) (TmPP)Co **1** and (b) $(NO_2TmPP)Co$ **3** in CH_2Cl_2 containing 0.1 M TBAP. Scan rate = 0.10 V s^{-1}.

Table 1. Half-wave potentials (V *vs* SCE) of cobalt porphyrins in CH_2Cl_2, 0.10 M TBAP

Compound	Ring-ox		Co^{III}/Co^{II}	Co^{II}/Co^{I}	Co^{III}-R red[a]	Ring-red	
(TmPP)Co **1**	1.15	0.96	0.72	-0.90[b]	-1.44[b]		
(TdmPP)Co **2**	1.16	0.96	0.74	-0.92[b]	-1.42[b]		
$(NO_2TmPP)Co$ **3**	1.28	1.05	0.80			-0.66	-1.32
$(NO_2TdmPP)Co$ **4**	1.33	1.11	0.83			-0.64	-1.30

[a]Reduction of the product, $(TRPP)Co^{III}(CH_2Cl)$, generated from the reaction between the cobalt(I) porphyrin and CH_2Cl_2. [b]Peak potential for irreversible reduction at a scan rate of 0.10 V/s.

Although two reductions are seen for the nitro and non-nitro substituted porphyrins, the reversibility and sites of electron transfer differ between the two types of porphyrins. As seen in Fig. 2, both reductions of (TmPP)Co **1** are *irreversible* and located at E_{pc} = -0.90 and -1.44 V in CH_2Cl_2 containing 0.10 M TBAP, while both reductions of $(NO_2TmPP)Co$ **3** are *reversible* and located at $E_{1/2}$ = -0.66 and -1.32 V.

It is well-documented in the literature that Co(II) porphyrins can undergo either a metal-centered reduction to give a Co(I) porphyrin or reduction at the conjugated π-system to give a Co(II) porphyrin π-anion radical, with the exact site depending upon the structure of the compound and solution conditions.[3] Most electrogenerated Co(I) porphyrins will react with CH_2Cl_2, which leads to an irreversible Co(II)/Co(I) reduction in this solvent.[3] This is the case for $(TmPP)Co^{II}$ **1** and $(TdmPP)Co^{II}$ **2**

which are assigned to metal-centered processes, leading to formation of a transient Co(I) product after the first one-electron reduction in CH_2Cl_2. This low valent complex is highly reactive and reacts with CH_2Cl_2 to generate a σ-bonded Co(III) product, $(TmPP)Co^{III}(CH_2Cl)$, as earlier described in the literature.[16,17] The *in-situ* generated σ-bonded porphyrin product is then further reduced at -1.44 V by one electron. Again, this is similar to what has been reported for other chemically and electrochemically generated σ-bonded $(TPP)Co^{III}(R)$ complexes, where R = CH_3, C_2H_5, C_3H_7 or CH_2Cl.[16,17]

The fact that a chemical reaction with CH_2Cl_2 does not occur for the nitro-substituted porphyrin **3** is consistent with the fact that the two reversible reductions both involve the conjugated porphyrin π-ring system and lead to generation of a Co(II) π-anion radical rather than a Co(I) porphyrin in the first step. Macrocycle ring-centered reductions of Co(II) porphyrins are not common but have previously been reported for a cobalt tetraphenylporphyrin with four CN groups at the β-pyrrole positions of the macrocycle.[18]

The easier reduction of **3** as compared to compound **1** is due in part to the substituent effect of the added nitro group and in part to the different sites of electron transfer. The absolute difference in peak potential between the first reduction of **1** and **3** is about 200 mV and a similar separation in peak potential is seen between the first reduction of compounds **2** and **4**. These values are in agreement with what has been reported for other nitro substituted porphyrins.[3]

UV-visible spectroelectrochemistry

In order to elucidate the site of electron transfer, the reduced and oxidized forms of compounds **1-4** were monitored by thin-layer UV-visible spectroelectrochemistry. Examples of the spectral changes which occurred during controlled potential reduction are shown in Fig. 3 while the changes during oxidation are shown in Fig. 4.

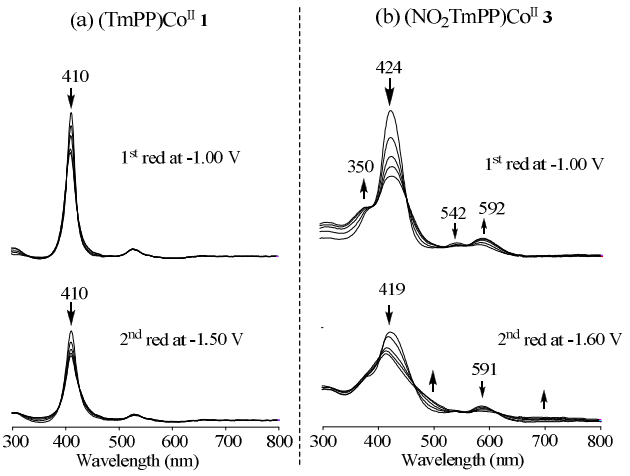

Fig. 3. Thin-layer UV-visible spectral changes of (a) $(TmPP)Co^{II}$ **1** and **(b)** $(NO_2TmPP)Co^{II}$ **3** during controlled potential reductions in CH_2Cl_2 containing 0.10 M TBAP

As seen in Fig. 3a, the intensity of the Soret and Q bands of compound **1** decrease only slightly upon the first one-electron reduction at -1.00 V in CH_2Cl_2 containing 0.1 M TBAP. The spectral changes are irreversible and the initial spectrum could not be generated when the potential was set back to 0.0 V for re-oxidation. This result is consistent with the first reduction occurring at the metal center to give a Co(I) porphyrin which then reacts with CH_2Cl_2 to generate a σ-bonded porphyrin, $(TmPP)Co^{III}(CH_2Cl)$. Thus, the initial spectrum before reduction is that of a Co(II) porphyrin and that after reduction is that of a Co(III) porphyrin. In contrast to compound **1**, the spectral changes during reduction of compound **3** are more significant (Fig. 3b). The Soret band initially at 424 nm decreases in intensity as the reduction proceeds consistent with formation of a Co(II) porphyrin π-anion radical. Further reduction at -1.60 V leads to additional loss of the Soret band intensity as the Co(II) dianion is generated in solution.

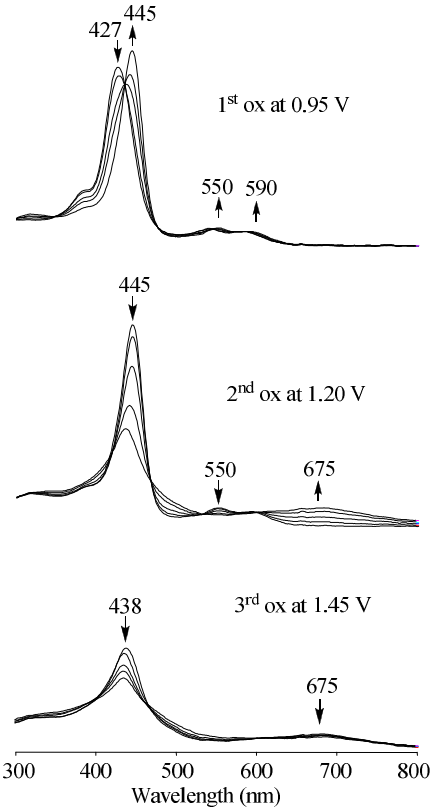

Fig. 4. Thin-layer UV-visible spectral changes of $(NO_2TdmPP)Co^{II}$ **4** during controlled potential oxidations in CH_2Cl_2 containing 0.10 M TBAP.

The first one-electron oxidation of $(NO_2TdmPP)Co^{II}$ **4** at 0.95 V results in a decreased intensity Soret band at 427 nm as a new Soret band grows in 445 nm. These spectral changes are shown in Fig. 4a and are consistent with a metal-centered electron transfer to give a Co(III) porphyrin during the first electron abstraction. In the second one-electron oxidation process, a new broad Q band appears at 675 nm while the Soret band at 445 nm decreases in intensity and is shifted to 438 nm, indicating generation of a Co(III) porphyrin π-cation radical in CH_2Cl_2. Similar spectral changes occur for compounds **1-3**. Similar spectral changes have also been reported for related porphyrins in non-aqueous media.[19-21]

Electrocatalytic reduction of oxygen

Each compound was examined as a catalyst for the electroreduction of oxygen when adsorbed on an EPPG disk in 1.0 M $HClO_4$. Examples of cyclic voltammograms showing the Co(III)/Co(II) reduction process in 1.0 M $HClO_4$ saturated with N_2 (-----) and saturated with air (—) are illustrated in Fig. 5.

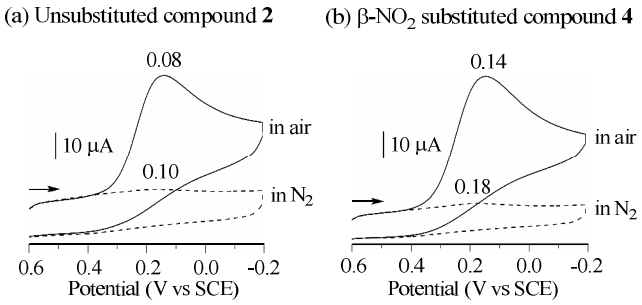

Fig. 5. Cyclic voltammorgams of (a) unsubstituted compound **2** and (b) β–pyrrole NO_2-substituted compound **4** absorbed on an EPPG electrode in 1.0 M $HClO_4$ under N_2 (---) and air (–). Scan rate is 50 mV·s^{-1}

The Co^{II}/Co^{III} (and Co^{III}/Co^{II}) processes of compounds **1-4** are reversible in CH_2Cl_2 and located at $E_{1/2}$ = 0.72-0.83 V (see Fig. 2). In contrast, the Co(III)/Co(II) reduction peaks of **1-4** are irreversible and located at similar potentials of +0.05 to +0.18 V in 1.0 M $HClO_4$ under N_2 or under O_2 (air). The negative shift in Co(III) reduction potential is due to strong coordination with the Co(III) central metal ion and the irreversibility of the process is due to coupled chemical reactions after electron transfer. The chemical reactions involve changes in coordination which has been demonstrated for many cobalt porphyrins in many different solvents.[3]

The magnitudes of the reduction peak currents under O_2 are much larger in the acid solutions which are saturated with air. The significant increase in the cathodic peak current in the presence of oxygen and the lack of a return peak on the reverse sweep of the cyclic voltammogram in air is characteristic for a catalytic reaction, which, in this case, is the catalytic reduction of O_2, either *via* a two-electron transfer process to give H_2O_2 or *via* a four-electron transfer process to give H_2O.

As seen in Fig. 5, both the unsubstituted compound **2** and the β-NO_2 substituted compound **4** act as catalysts for the reduction of O_2. The Co(III)/Co(II) reduction peak potential of the β-pyrrole NO_2 substituted compound **4** is located at +0.18 V under N_2 and is positively shifted by 80 mV as compared to the peak potential of +0.10 V for compound **2** (see dashed lines in Fig.5). The peak potential of **4** (+0.14 V) in air saturated solution is also positively shifted by 60 mV as compared to the E_p (+0.08 V) for the unsubstituted compound **2**.

The product formed in the catalytic reduction of O_2 (H_2O_2 or H_2O) and the number of electrons transferred in the reduction of dioxygen was calculated from the magnitude of the steady-state limiting currents that were taken at a fixed potential (−0.10 V) on the plateau of the catalytic wave of the current-voltage curve. Examples of the current-voltage curves are shown in Fig. 6 along with the related Koutecky-Levich plots. The slope of the plot obtained by linear regression was then used to estimate the average number of electrons (n) involved in the catalytic reduction of O_2.[22] The Koutecky-Levich plot is interpreted on the basis of equation 1,[23] where j is the measured limiting current density (mA·cm^{-2}), j_{lev} is the Levich currents, the j_k is the kinetic current which are defined by equations 2 and 3.[24]

$$1/j = 1/j_{lev} + 1/j_k \quad (1)$$

$$j_{lev} = 0.62nFD^{2/3}c^*v^{-1/6}\omega^{1/2} \quad (2)$$

$$j_k = 10^3knF\Gamma c^* \quad (3)$$

The n in equation 3 represents the number of electrons transferred in the overall electrode reaction, F *is* the Faraday constant (96,485 C·mol^{-1}), D and c^* are the diffusion coefficient (cm^2·s^{-1}) and bulk concentration of O_2 in 1.0 M $HClO_4$, v is the kinematic viscosity of water, ω is the angular rotation speed (rad·s^{-1}) of the electrode, k is the second order rate constant of the reaction (mol^{-1}·L·s^{-1}) and the Γ is the surface concentration of porphyrins (mol·cm^{-2}).

The catalytic reduction of oxygen by metalloporphyrins or metallocorroles adsorbed on an electrode surface can proceed via a two-electron transfer pathway to generate hydrogen peroxide, or via a direct four-electron pathway to give H_2O. Any H_2O_2 produced can be further reduced to H_2O and, when this occurs, the number of electrons transferred (n) during the reduction of oxygen could be between 2 and 4.[12,13,25,26]

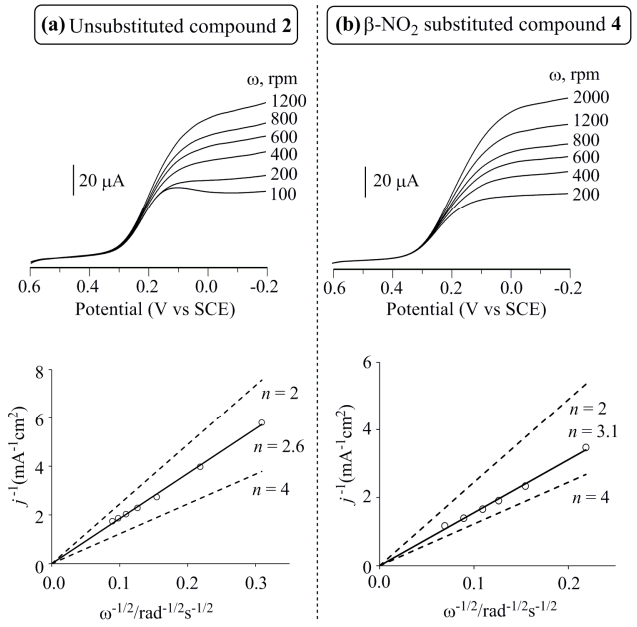

Fig. 6. Current-voltage curves and Koutecky-Levich plots for catalytic reduction of O_2 in 1.0 M $HClO_4$ saturated with air at a rotating EPPG disk electrode coated with (a) unsubstituted compound **2** and (b) β-pyrrole NO_2-substituted compound **4**. Electrode rotating rates (ω) are indicated on each curve. Potential scan rate = 50 mV·s^{-1}.

The calculated number of electrons transferred (n) to O_2 in the electroreduction process using compounds **1-4** as catalysts and the corresponding percentage of the H_2O_2 product is given in Table 2. A two electrons transfer (n = 2) would generate 100% H_2O_2 and a four electrons transfer (n = 4) would give 0% H_2O_2 and 100% H_2O. The experimentally determined n values range from 2.6 to 3.1 which corresponds to 70-45% H_2O_2 (and 30-55%

H_2O) produced. The values of n for compounds **3** and **4** (n = 3.1) are larger than that for compounds **1** and **2** (n = 2.6-2.8), indicating that the β-pyrrole nitro-substituted compounds are better catalysts than the non-nitro substituted porphyrins for the electroreduction of oxygen in acid media.

Table 2. Potentials (V vs SCE) of cobalt porphyrins in 1.0 M $HClO_4$.

Compound	E_{pc} without O_2	E_{pc} with O_2	n	H_2O_2%
(TmPP)Co **1**	0.07	0.05	2.8	60
(TdmPP)Co **2**	0.10	0.08	2.6	70
(NO_2TmPP)Co **3**	0.16	0.14	3.1	45
(NO_2TdmPP)Co **4**	0.18	0.14	3.1	45

Conclusions

In summary, four substituted cobalt(II) porphyrins were synthesized and examined as to their electrochemistry and catalytic properties for the reduction of molecular oxygen. The strong electron-withdrawing nitro-substituent on a β-pyrrole position of the porphyrin macrocycle is shown to have a significant effect on the UV-visible spectra, redox potentials and reduction mechanism in nonaqueous media. As seen in this study, the nitro group also affects the catalytic efficiency of the compounds. The β-pyrrole NO_2-substituted cobalt porphyrins are the better electrocatalysts than the non-nitro substituted derivatives for the reduction of molecular oxygen in acid media.

Acknowledgements

We gratefully acknowledge supports from the Natural Science Foundation of China (No. 21071067) and the Robert A. Welch Foundation (K.M.K., Grant E-680).

Notes and references

[a]*School of Chemistry and Chemical Engineering, Jiangsu University, Zhenjiang P. R. China.. Fax: +86 511 88791800; Tel: +86 511 88791800; E-mail: zpou2003@yahoo.com*
[b]*Department of Chemistry, University of Houston, Houston, Texas, USA. 77204-5003. Fax: 01 713 7432745; Tel: 01 713 7432740; E-mail: kkadish@uh.edu*

1 *Handbook of Porphyrin Science*, ed. K. M. Kadish, K. M. Smith and R. Guilard, World Scientific, New Jersey, 2010, Vol. 10-12, 18, 21.
2 *The Porphyrin Handbook*, ed. K. M. Kadish, K. M. Smith and R. Guilard, Academic Press, San Diego, 2000, Vol. 6, pp 1-340.
3 K. M. Kadish, E. Van Caemelbecke and G. Royal, In *The Porphyrin Handbook*, ed. K. M. Kadish, K. M. Smith and R. Guilard, Academic Press, New York, 2000, Vol. 8, Ch. 55, pp 1-144.
4 T. S. Shi, H. Sun, X. Cao and J. Tao, *Chem. J. Chinese Univ*., 1994, **15**, 966-969.
5 J. Z. Tao, H. Sun, T. Shi and X. Cao, *Chem. J. Chinese Univ*., 1994, **15**, 1657-1661.
6 K. M. Kadish, W. E, P. J. Sintic, Z. P. Ou, J. G. Shao, K. Ohkubo, S. Fukuzumi, L. J. Govenlock, J. A. McDonald, A. C. Try, Z. Cai, J. R. Reimers and M. J. Crossley, *J. Phys. Chem. B* , 2007, **111**, 8762-8774.
7 B. H. Li, Z. P. Ou, D. Y. Meng, J. J. Tang, Y. Y. Fang, R. Liu and K. M. Kadish, *J. Inorg. Biochem.,* 2014, in press, online Jan. 14, 2014. Http://dx.doi.org/10.1016/j.jinorgbio. 2013.12. 014.
8 S. Nardis, M. Stefanelli, P. Mohite, G. Pomarico, L. Tortora, M. Manowong, P. Chen, K. M. Kadish, F. R. Fronczek, G. T. McCandless, K. M. Smith and R. Paolesse, *Inorg. Chem.,* 2012, **51**, 3910-3920.
9 D. Bhattacharya, P. Singh and S. Sarkar, *Inorg. Chim. Acta*, 2010, **363**, 4313-4318.
10 Z. Ou, K. M. Kadish, W. E, J. Shao, P. J. Sintic, K. Ohkubo, S. Fukuzumi and M. J. Crossley, *Inorg. Chem.,* 2004, **43**, 2078-2086.
11 S. B. Yang, B. Sun, Z. P. Ou, D. Y. Meng, G. F. Lu, Y. Y. Fang and K. M. Kadish, *J. Porphyrins Phthalocyanines*, 2013, **17**, 857-869.
12 A. X. Lü, Y. Y. Fang, M. Zhu, S. Huang, Z. P. Ou and K. M. Kadish, *J. Porphyrins Phthalocyanines,* 2012, **16**, 310-315.
13 Z. P. Ou, A. X. Lü, D. Y. Meng, S. Huang, Y. Y. Fang, G. F. Lu and K. M. Kadish, *Inorg. Chem*., 2012, **51**, 8890-8896.
14 C. N. Shi and F. C. Anson, *Inorg. Chem*., 1998, **37**, 1037-1043.
15 A. Giraudeau, H. J. Callot, J. Jordan, I. Ezhar and M. Gross, M. *J. Am. Chem. Soc*., 1979, **101**, 3857 -3862.
16 K. M. Kadish, B. C. Han and A. Endo, *Inorg. Chem.,* 1991, **30**, 4502-4506.
17 G. Maiya, B. C. Han and K. M. Kadish, *Langmuir,* 1989, **5**, 645-650.
18 X. Lin, B. Boisselier-Cocolios and K.M. Kadish. *Inorg. Chem.,* 1986, **25,** 3242-3248.
19 K. M. Kadish, J. Li, E. Van Caemelbecke, Z. P. Ou, N. Guo, M. Autret, F. D'Souza and P. Tagliatesta, *Inorg. Chem.,* 1997, **36**, 6292-6298.
20 F. D'Souza, A. Villard, E. Van Caemelbecke, M. Franzen, T. Boschi, P. Tagliatesta and K. M. Kadish, *Inorg. Chem*., 1993, **32**, 4042-4048.
21 W. H. Zhu, M. Sintic, Z. P. Ou, P. J. Sintic, J. A. McDonald, P. R. Brotherhood, M. J. Crossley and K. M. Kadish, *Inorg. Chem.,* 2010, **49**, 1027-1038.
22 S. Treimer, A. Tang and D. C. Johnson, *Electroanalysis,* 2002, **14**, 165-171.
23 N. Oyama and F. C. Anson, *Anal. Chem*., 1980, **52**, 1192-1198.
24 *Electrochemical Methods: Fundamentals and Applications*, 2nd ed. A. J. Bard and L. T. Faulkner, John Wiley & Sons, New York, 2001.
25 C. M. Lemon, D. K. Dogutan and D. G. Nocera. In *Handbook of Porphyrin Science*, ed. K. M. Kadish, K. M. Smith and R. Guilard, World Scientific, New Jersey, 2012, Vol. 21, pp. 1-143.
26 A. Schechter, M. Stanevsky, A. Mahammed, Z. Gross, *Inorg. Chem*., 2012, **51**, 22-24.

Synopsis

Synthesis and electrochemistry of β-pyrrole nitro-substituted cobalt(II) porphyrins. Effect of the NO_2 group on redox potentials, electron transfer mechanism and catalytic reduction of molecular oxygen in acid media

Bin Sun, Zhongping Ou,* Shuibo Yang, Deying Meng, Guifen Lu, Yuanyuan Fang and Karl M. Kadish*

Four cobalt porphyrins were synthesized and characterized as to their electrochemical and spectroelectrochemical properties. The electrocatalytic activity of each porphyrin for reduction of molecular oxygen when coated on an edge-plane pyrolytic graphite electrode was also examined in acid media.

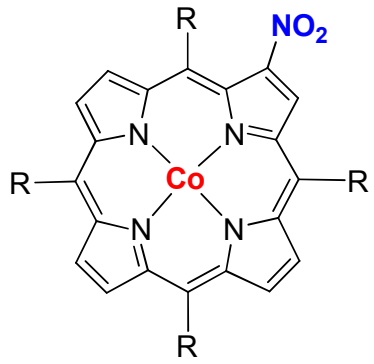

R = 4-CH_3Ph or 3,5-$(OCH_3)_2$Ph